UNIVERSIDADE DE SÃO PAULO

PUBLICAÇÕES

SIGNAL AND BACKGROUNDS FOR LEPTOQUARKS AT THE LHC

O.J.P. Éboli and **R.Z. Funchal**
Instituto de Física, Universidade de São Paulo

T.L. Lungov
Fermi National Accelerator Laboratory
P.O. Box 500, Batavia, IL 60510, USA

Agosto/97

Pág. 1 - 37

Signal and Backgrounds for Leptoquarks at the LHC

O. J. P. Éboli[*], R. Z. Funchal[†],

Instituto de Física, Universidade de São Paulo

C.P. 66.318, 05315-970 São Paulo, Brazil

T. L. Lungov[‡]

Fermi National Accelerator Laboratory

P.O. Box 500, Batavia, IL 60510, USA

(August 29, 1997)

Abstract

We study the potentiality of the CERN Large Hadron Collider (LHC) to unravel the existence of first generation scalar leptoquarks. Working with the most general $SU(2)_L \otimes U(1)_Y$ invariant leptoquark interactions, we analyze in detail the signals and backgrounds that lead to a final state containing a pair e^+e^- and jets. Our results indicate that a machine like the LHC will be able to discover leptoquarks with masses up to 2–3 TeV depending on their couplings.

[*]Email: eboli@fma.if.usp.br

[†]Email: zukanov@charme.if.usp.br

[‡]Email: lungov@fnal.gov

1

I. INTRODUCTION

Many extensions of the Standard Model (SM) treat quarks and leptons in the same basis and, consequently, allow the existence of particles, called leptoquarks, that mediate quark-lepton transitions. The class of theories exhibiting these particles includes composite models [1,2], grand unified theories [3], technicolor models [4], and superstring-inspired models [5]. Leptoquarks carry simultaneously leptonic and baryonic number, and can have spin 0 or 1.

Since leptoquarks are an undeniable signal of physics beyond the SM, there have been several direct searches for them in accelerators. So far, all searches led to a negative result, with the possible exception of some intriguing events in e^+p collisions at HERA [6]. Analyzing the decay of the Z into a pair of on-shell leptoquarks, the LEP experiments established a lower bound $M_{lq} \gtrsim 44$ GeV for scalar leptoquarks [7,8]. This limit can be improved by looking for Z decays into an on-shell leptoquark and an off-shell one, resulting in $M_{lq} \gtrsim 65 - 73$ GeV [8]. The search for scalar leptoquarks decaying exclusively into electron-jet pairs at the Tevatron constrained their masses to be $M_{lq} \gtrsim 225$ GeV [9]. Furthermore, the experiments at HERA [10] placed limits on their masses and couplings, establishing that $M_{lq} \gtrsim 216 - 275$ GeV depending on the leptoquark type and couplings.

The direct search for leptoquarks with masses above a few hundred GeV can be carried out only in the next generation of colliders. There have been many studies of the production of leptoquarks in the future pp [11], ep [12,13], e^+e^- [14], e^-e^- [15], $e\gamma$ [16], and $\gamma\gamma$ [17] colliders. In this work, we study the capability of the CERN Large Hadron Collider (LHC) to unravel the existence of scalar leptoquarks through the final state topology two jets plus a pair e^+e^-. This is accomplished by a careful analyses of the signal and its respective backgrounds. We performed our analyses for first generation leptoquarks that couple to pairs e^-u, e^+u, e^-d, or e^+d with the leptoquark interactions described by the most general effective Lagrangian that is invariant under $SU(3)_C \otimes SU(2)_L \otimes U(1)_Y$ [12].

It is interesting to notice that pair production of scalar leptoquarks in a hadronic collider is essentially model independent since the leptoquark–gluon interaction is fixed by the

$SU(3)_C$ gauge invariance. On the other hand, single production is model dependent because it takes place via unknown interactions. Notwithstanding, these two signals are complementary because they allow us not only to reveal their existence but also to determine their properties such as mass and Yukawa couplings to quarks and leptons.

The single and pair productions of leptoquarks can give rise to jets accompanied by e^+e^- pairs. In this work, we performed a careful analyses of all possible QCD and electroweak backgrounds for the jets plus a e^+e^- pair topology using the event generator PYTHIA version 5.7 [18], taking into account initial and final state QCD radiation. The signal was also generated using this package. We devised a series of cuts not only to reduce the background and enhance the signal but also to separate the single and pair production mechanisms. Our analyses improves the previous ones [19] since we considered all possible backgrounds as well as the most general model for leptoquarks.

We analyzed the single leptoquark production taking into account the contribution from pair production, which enhances the signal, and we obtained exclusion regions in terms of the leptoquark mass and Yukawa coupling. With a luminosity of 10 (100) fb^{-1} and a center-of-mass energy of 14 TeV, the single leptoquark search at the LHC can exclude their existence at 95% CL for masses smaller than 1.3–1.5 (1.7–2.0) TeV irrespective of their Yukawa couplings. For larger masses, the LHC reach depends on the coupling of the leptoquark to fermions. On the other hand, the production of a leptoquark pair can be observed up to masses of 1.1–1.3 (1.5–1.7) TeV depending only upon the leptoquark type.

Low-energy experiments lead to strong indirect bounds on the couplings and masses of leptoquarks, which can be used to define the goals of new machines to search for these particles. The main sources of indirect constraints are:

• Leptoquarks give rise to Flavor Changing Neutral Current (FCNC) processes if they couple to more than one family of quarks or leptons [20,21]. In order to avoid strong bounds from FCNC, we assumed that the leptoquarks couple to a single generation of quarks and a single one of leptons. However, due to mixing effects on the quark sector, there is still some amount of FCNC left [22] and, therefore, leptoquarks that couple to the first two generations

3

of quarks must comply with some low-energy bounds [22].

- The analyses of the decays of pseudoscalar mesons, like the pions, put stringent bounds on leptoquarks unless their coupling is chiral – that is, it is either left-handed or right-handed [20].

- Leptoquarks that couple to the first family of quarks and leptons are strongly constrained by atomic parity violation [23]. In this case, there is no choice of couplings that avoids the strong limits.

- The analyses of the effects of leptoquarks on the Z physics through radiative corrections lead to limits on the masses and couplings of leptoquarks that couple to top quarks [24,25].

As a rule of a thumb, the low-energy data constrain the masses of leptoquarks to be larger than 0.5—1 TeV when their Yukawa coupling is equal to the electromagnetic coupling e [22,25,26]. Therefore, our results indicate that the LHC can confirm these indirect limits and also expand them considerably.

The outline of this paper is as follows. In Sec. II we introduce the $SU(2)_L \otimes U(1)_Y$ invariant effective Lagrangians that we analyzed and its connection to the production cross sections used in PYTHIA. A detailed discussion of all possible backgrounds is exhibited in Sec. III, while Sec. IV contains the main features of the signals for single and double leptoquark productions. Our analyses are shown in Sec. V and we draw our conclusions in Sec. VI.

II. MODELS FOR SCALAR LEPTOQUARK INTERACTIONS

A natural hypothesis for theories beyond the SM is that they exhibit the gauge symmetry $SU(2)_L \otimes U(1)_Y$ above the electroweak symmetry breaking scale v, therefore, we imposed this symmetry on the leptoquark interactions. In order to avoid strong bounds coming from the proton lifetime experiments, we required baryon (B) and lepton (L) number conservation, which forbids the leptoquarks to couple to diquarks. The most general effective Lagrangian for leptoquarks satisfying the above requirements and electric charge and color conservation

is given by [12]

$$\mathcal{L}_{\text{eff}} = \mathcal{L}_{F=2} + \mathcal{L}_{F=0} , \tag{1}$$

$$\mathcal{L}_{F=2} = g_{1L} \, \bar{q}_L^c \, i\tau_2 \, \ell_L \, S_{1L} + g_{1R} \, \bar{u}_R^c \, e_R \, S_{1R} + \tilde{g}_{1R} \, \bar{d}_R^c \, e_R \, \tilde{S}_1 + g_{3L} \, \bar{q}_L^c \, i\tau_2 \, \vec{\tau} \, \ell_L \cdot \vec{S}_3 , \tag{2}$$

$$\mathcal{L}_{F=0} = h_{2L} \, R_{2L}^T \, \bar{u}_R \, i\tau_2 \, \ell_L + h_{2R} \, \bar{q}_L \, e_R \, R_{2R} + \tilde{h}_{2L} \, \tilde{R}_2^T \, \bar{d}_R \, i\tau_2 \, \ell_L , \tag{3}$$

where $F = 3B + L$, q (ℓ) stands for the left-handed quark (lepton) doublet, and u_R, d_R, and e_R are the singlet components of the fermions. We denote the charge conjugated fermion fields by $\psi^c = C\bar{\psi}^T$ and we omitted in Eqs. (2) and (3) the flavor indices of the leptoquark couplings to fermions. The leptoquarks $S_{1R(L)}$ and $\tilde{S}_1$ are singlets under $SU(2)_L$, while $R_{2R(L)}$ and $\tilde{R}_2$ are doublets, and S_3 is a triplet. The quantum numbers for all scalar leptoquarks can be found, for instance, in the last reference of [14]. Since leptoquarks are color triplets, it is natural to assume that they interact with gluons. To obtain their couplings to gluons we substituted ∂_μ by the covariant derivative $D_\mu = \partial_\mu + ig_s \lambda_{jk}^a G_\mu^a / 2$ in the leptoquark kinetic Lagrangian.

From the above interactions we can see that the main decay modes of leptoquarks are into pairs $e^\pm q$ and $\nu_e q'$, thus, their signal is a $e^\pm$ plus a jet, or a jet plus missing energy. In this work we considered only the first decay and took into account properly the corresponding branching ratio. Moreover, the event generator PYTHIA assumes that the leptoquark interaction with quarks and leptons is described by

$$\bar{e}(a + b\gamma_5)q , \tag{4}$$

and the cross sections are expressed in terms of the parameter κ defined as

$$\kappa \alpha_{\text{em}} \equiv \frac{a^2 + b^2}{4\pi} \tag{5}$$

with α_{em} being the fine structure constant. We exhibit in Table I the leptoquarks that can be analyzed using the final state $e^\pm$ plus a jet, as well as, their decay products, branching ratio into $e^\pm q$, and the correspondent value of κ. As we can see from Eqs. (2) and (3), only the leptoquarks R_{2L}^2, $\tilde{R}_2^2$ and S_3^- decay exclusively into a jet and a neutrino.

5

At the parton level, the single production of leptoquarks leads to a final state exhibiting a pair e^+e^- and q ($\bar{q}$). After the parton shower and hadronization the final state usually contains more than one jet, and consequently, the backgrounds for single and pair productions of leptoquarks are basically the same. In our analyses we kept track of the $e^\pm$ (jet) carrying the largest transverse momentum, that we denoted by e_1 (j_1), and the $e^\pm$ (jet) with the second largest p_T, that we called e_2 (j_2). The reconstruction of the jets in the final state was done using the subroutine LUCELL of PYTHIA, requiring the transverse energy of the jet to be larger than 7 GeV inside a cone $\Delta R = \sqrt{\Delta\eta^2 + \Delta\phi^2} = 0.7$. Our calculations were performed using the parton distribution functions of CTEQ2L [27].

Within the scope of the SM, there are many sources of backgrounds leading to jets accompanied by a pair e^+e^-. We divided them into three classes: QCD and electroweak processes and top quark production.

A. QCD processes

The reactions, included in the QCD class, depend exclusively on the strong interaction and are listed in Table II, where q ($\bar{q}$) represents a (anti)quark of flavor u, d, c, s, or b and g stands for a gluon. We also show in this table the total cross section (σ_{bare}) for each process with the only requirement that the partons produced in the hard scattering have a transverse momentum larger than 100 GeV [28]. The last column in this table contains the total cross section (σ_{pair}) after imposing that the final state contains a pair e^+e^- with each lepton having a transverse momentum larger than 50 GeV.

In this class of processes, the main source of hard $e^\pm$ is the semileptonic decay of hadrons possessing quarks c or b, which are produced in the hard scattering or in the parton shower through the splitting $g \rightarrow c\bar{c}$ ($b\bar{b}$). Since only a small fraction of the decays give rise to hard leptons, we needed to improve the efficiency of the Monte Carlo by decaying the

6

same hadron several times and keeping track of the fraction of events that yield the desired signal. An important feature of the events in this class is that close to the hard $e^{\pm}$ there is a substantial amount of hadronic activity, as we can see from Fig. 1, where we show the hadronic transverse energy deposited in a cone of size $R = \sqrt{\Delta\eta^2 + \Delta\phi^2} = 0.7$ around the $e^{\pm}$ direction.

We show in Fig. 2 the p_T spectrum of the $e^{\pm}$ and jets with the largest transverse momenta. As we can see from this figure, the processes in this class yield a large number of jets with large transverse momentum, however, the p_T of the second most energetic $e^{\pm}$ (e_2) is seldom larger than 200 GeV. From Fig. 3a we can learn the $e_1 e_2$ invariant mass distribution is peaked at small masses, however it still has a sizable value up to invariant masses of the order of 400 GeV. We can assess the importance of this background from the invariant mass spectrum of lepton-jet pairs that is shown in Fig. 3b, where we added the contributions from all e_i–j_k pairs $(i, k = 1, 2)$.

B. Electroweak processes

The electroweak class contains the Drell-Yan production of quark pairs and the single and pair productions of electroweak gauge bosons. We list in Table III all processes included into this class and respective cross sections (σ_{bare} and σ_{pair}) evaluated with the same cuts applied to the QCD processes. It is interesting to notice that the reaction $q_i g \to q_i Z$ is the dominant background with the minimal cuts applied so far. Moreover, the majority of the $e^{\pm}$ produced by this class of processes originates from the decay of an electroweak gauge boson, and consequently they tend to be isolated, as we can see from Fig. 4.

We exhibit in Fig. 5 the p_T spectrum of the $e^{\pm}$ and jets, which shows that this class of events yields leptons with larger transverse momentum than the QCD class, while the jets have smaller p_T. From Fig. 6a we can learn that the $e_1 e_2$ invariant mass distribution is peaked around the Z mass and its is non-negligible up to invariant masses of the order of 400 GeV. We plot in Fig. 6b the sum of all e_i–j_k invariant masses, which indicates that the

7

importance of these background processes decrease for heavier leptoquarks.

C. Top production

The production of top quark pairs takes place through quark and gluon fusion, being the last one the dominating process at the LHC energy due to the large gluon-gluon luminosity. We list in Table IV the cross sections σ_{bare} and σ_{pair} evaluated with the same cuts used for the QCD processes and assuming the top mass to be 174 GeV. As we can see from this table, top quark pairs will be copiously produced at LHC, being the top quark production one of the largest backgrounds before applying further cuts. Moreover, the $e^{\pm}$ produced in the top decay into $be\nu_e$ channel are rather isolated, as shown in Fig. 7.

We present the p_T spectrum of the jets and $e^{\pm}$ in Fig. 8. As we can see, this distribution is peaked towards low transverse momenta and contains high p_T leptons (jets) up to 500 (900) GeV. The invariant mass of the $e_1 e_2$ pairs generated in top decays reaches a maximum around 400 GeV and extends up to 1300 GeV, as we can see from Fig. 9a. From the distribution of e_i–j_k invariant masses, shown in Fig. 9b, we can see that this processes can give rise to background events even for leptoquarks with masses in the TeV range.

IV. SIGNALS FOR THE PRODUCTION OF LEPTOQUARKS

In hadronic colliders, leptoquarks can be single or pair produced through the processes

$$q + g \rightarrow S_{\text{lq}} + \ell \ , \tag{6}$$

$$q + \bar{q} \rightarrow S_{\text{lq}} + \bar{S}_{\text{lq}} \ , \tag{7}$$

$$g + g \rightarrow S_{\text{lq}} + \bar{S}_{\text{lq}} \ , \tag{8}$$

where $\ell = e^{\pm}$ (ν) and we denoted the scalar leptoquark by S_{lq}. In this work we focus our attention on the case that ℓ is a charged lepton. When the leptoquark decays into a $e^{\pm}$–q pair, the final state presents a pair $e^+ e^-$ and jets after hadronization. The cross sections for pair production are model independent because the leptoquark–gluon interaction

8

is determined by the $SU(3)_C$ gauge invariance. On the other hand, the single production is model dependent once it involves the the unknown Yukawa coupling of leptoquarks to a lepton–quark pairs.

A. Single production

The cross section for the associated production of a leptoquark and a charged lepton, process (6), depends quadratically on the parameter κ defined in Eq. (5). We exhibit in Table V the total cross section for the production of a leptoquark (σ_{pair}) that couples only to a charged lepton and a quark, assuming $\kappa = 1$ and requiring that the $e^{\pm}$ have transverse momenta larger than 50 GeV. As could be anticipated from the effective Lagrangian (1), the cross sections for the production of $e^+ q$ and $e^- q$ leptoquarks are equal. Furthermore, it is interesting to notice that the cross section for the production of a leptoquark coupling only to u quarks is approximately twice the one of leptoquarks coupling only to d quarks, in agreement with a naive valence-quark-counting rule.

In what follows, we show several kinematical distributions for leptoquarks that couple only to $e^+ \bar{u}$ pairs and mass $M_{\text{lq}} = 1$ TeV, however, the distributions for other leptoquarks are very similar. As expected, the bulk of the $e^{\pm}$ originating from the single (and also pair) production of leptoquarks are isolated, as we can see from Fig. 10. We plot in Fig. 11 the p_T spectrum of the leptons $e_{1(2)}$ and jets $j_{1(2)}$. Notice that the p_T spectrums of the most energetic jet and $e^{\pm}$ peak around $M_{\text{lq}}/2$ ($\simeq$ 500 GeV), which indicates that the $e^{\pm}$ and jet resulting from the leptoquark decay are often the ones with the largest transverse momentum in the case of single leptoquark production. Contrary to what we have seen in the background processes, the single leptoquark production leads to $e^{\pm}$ with large transverse momenta.

Fig. 12a shows the invariant mass distribution of the lepton pair $e_1 e_2$, which is peaked toward low invariant masses and it extends up to very large invariant masses. This feature is important to reduce the backgrounds, specially the on-shell production of Z's. Furthermore,

9

the signal for the production of leptoquarks is a peak in the invariant mass (M_{ik}) of e_i–j_k pair at M_{lq} ($= 1$ TeV) which can be easily seen in Fig. 12b.

B. Pair production

The pair production of leptoquarks takes place through quark–quark and gluon–gluon fusions [Eqs. (7) and (8)], which rely exclusively on the color gauge interactions of the leptoquarks, and consequently they do not depend on the leptoquark species. As we can see from Table VI, the gluon–gluon mechanism dominates the production of leptoquark pairs as long as the signal is observable at the LHC. Moreover, for $\kappa = 1$, the cross section for the production of leptoquark pairs is larger than the single production one for light leptoquarks ($M_{lq} \lesssim 500$ GeV) due to the large gluon–gluon luminosity.

The transverse momentum distributions of the $e_{1(2)}$ and $j_{1(2)}$ are shown in Fig. 13, where we just required the $e^\pm$ to have $p_T > 50$ GeV. We can see from this figure that the $q\bar{q}$ and gg processes lead to a similar spectrum that is peaked approximately at $M_{lq}/2$ ($= 500$ GeV) and also exhibits a large fraction of very hard jets and leptons. The presence of this peak indicates that the two hardest jets and leptons originate from the decay of the leptoquark pair. However, we still have to determine which are the lepton and jet coming from the decay of one of the leptoquarks.

The invariant mass of pairs e^+e^- is usually quite large as shown in Fig. 14a, and we verified that the invariant mass spectrum of the $j_1 j_2$ pairs is similar to the e^+e^- one. There is a clear peak in the invariant mass (M_{ik}) distribution of e_i–j_k pairs, as shown in Fig. 14b.

V. RESULTS

There are several goals in our analyses. First, we study the LHC potentiality to discover a leptoquark, which requires establishing the cuts to enhance the signal and reduce the backgrounds. Then, we separate the single and pair productions of leptoquarks in order to be able to analyze their Yukawa couplings.

10

Taking into account the features of the signal and backgrounds described in the previous sections, we imposed the following set of cuts:

(C1) The first requirement is that the leading jets and $e^{\pm}$ are in the pseudorapidity interval $|\eta| < 3$.

(C2) The leading leptons (e_1 and e_2) should have $p_T > 200$ GeV.

(C3) We reject events where the invariant mass of the pair $e^+ e^-$ ($M_{e_1 e_2}$) is smaller than 190 GeV. This cut reduces the backgrounds coming from Z decays into a pair $e^+ e^-$.

(C4) In order to further reduce the $t\bar{t}$ and remaining off-shell Z backgrounds [29], we required that *all* the invariant masses $M_{e_i j_k}$ are larger than 200 GeV, since pairs $e_i j_k$ coming from an on-shell top decay have invariant masses smaller than m_{top}. The present experiments are able to search for leptoquarks with masses smaller than 200 GeV, therefore, this cut is in agreement with the present bounds.

In principle we should also require the $e^{\pm}$ to be isolated from hadronic activity in order to reduce the QCD backgrounds. Nevertheless, we verified that our results do not change when we introduced typical isolation cuts in addition to any of the above cuts. In fact, the cuts C1 and C2 eliminate all the QCD processes, except for $gg \rightarrow q\bar{q}$, for which 0.25% of the events survive the cuts C1 and C2 (and also C3). However, this background disappears when we apply C4.

We exhibit in Table III the fraction of electroweak events that passes the cuts C1, C2, and C3. As we can see from this table, the electroweak backgrounds associated to the production of a Z or a $W^+ W^-$ pair survive the cuts C1 and C2 and they are not completely eliminated even when we apply the cut C3. At this point, the most important backgrounds in this class are the production of a Z in association with a quark or a gluon, which have cross sections of the order of a few fb. Analogously to the QCD events, the electroweak backgrounds disappear after imposing C4.

11

A substantial fraction of the top backgrounds passes the cuts C1 and C2, as we can see from Table IV. The e^+e^- invariant mass cut (C3) reduces these backgrounds, however, they remain rather large, being of the order of 50 fb. When the C4 cut is applied, the only events that pass all cuts stem from $gg \to t\bar{t}$; nevertheless, the cross section of this process is smaller than 10^{-3} fb when we integrate in an invariant mass bin around a leptoquark mass; see below.

Since the cuts C1—C4 effectively suppress all the backgrounds to leptoquark production at the LHC, the leptoquark searches are free of backgrounds. Therefore, the LHC will be able to exclude with 95% CL the regions of parameter space where the number of expected signal events is larger than 3 for a given integrated luminosity.

A. Leptoquark pair search

In our analysis of leptoquark pair production we applied the cuts C1—C4 and also demanded the events to exhibit two e-jet pairs with a invariant masses in the range $|M_{lq} \pm \Delta M|$ with ΔM given in Table VII. The limits on the leptoquarks depend exclusively on its branching ratio into a charged lepton and jet (β) since they are produced by strong interaction processes that are the same for all leptoquark species. We show in Table VIII the 95% CL limits on the leptoquark masses that can be obtained from their pair production at the LHC for two different integrated luminosities. As we can see, this search will be able to exclude leptoquarks with masses up to 1.5 (1.7) TeV for $\beta = 0.5$ (1) and an integrated luminosity of 100 fb^{-1}, increasing considerably the present bounds.

B. Single leptoquark search

We also analyzed the search for leptoquarks through the existence of an excess of events presenting a e-jet invariant mass in the range $|M_{lq} \pm \Delta M|$ after we imposed the cuts C1—C4; see Table VII for ΔM. These events originate from the single production of leptoquarks, as well as their pair production, consequently having a larger cross section than the pair

12

or single production alone, and then increasing the reach of the LHC. However, this search is model dependent since the single production involves the couplings of the leptoquark to fermions. In fact, the cross section is determined by κ, β, and the quark that the leptoquark couples to. Therefore, for fixed κ, the production cross sections for leptoquarks S_{1L} and S_3^0 [$(S_{1R}, R_{2L}^1, \text{ and } R_{2R}^1)$ or $(S_3^+, R_{2R}^2, \tilde{R}_2^1, \text{ and } \tilde{S}_{1R})$] are equal.

Fig. 15 contains the 95% CL excluded regions in the plane κ–M_{lq} from the single leptoquark search. As expected, the excluded region is independent of κ for masses up to the reach of the leptoquark pair searches; see Table VIII. At higher masses the signal is dominated by the single production and consequently the bounds on leptoquarks that couple to d quarks (S_3^+, R_{2R}^2, $\tilde{R}_2^1$, and $\tilde{S}_{1R}$) are the weakest ones for a fixed value of κ. Since the leptoquarks S_{1R}, R_{2L}^1, and R_{2R}^1 couple to u quarks and have $\beta = 1$ they are the ones that possesses the most stringent limits. In fact, for leptoquark Yukawa couplings of the electromagnetic strength ($\kappa = 1$) and an integrated luminosity of 100 fb^{-1}, the LHC can exclude S_{1L} and S_3^0 leptoquarks with masses smaller than 2.6 TeV; while S_3^+, R_{2R}^2, $\tilde{R}_2^1$, and $\tilde{S}_{1R}$ leptoquarks with masses smaller than 2.4 TeV can be ruled out; and S_{1R}, R_{2L}^1, and R_{2R}^1 leptoquarks can be excluded up to masses of 2.9 TeV.

VI. CONCLUSIONS

The discover of leptoquarks is without any doubt a striking signal for the existence of life beyond the standard model. The LHC will be able to discover leptoquarks with masses smaller than 1.5–1.7 TeV irrespective of their Yukawa couplings through their pair production for an integrated luminosity of 100 fb^{-1}. Furthermore, the single leptoquark search can extend the reach of the LHC, allowing the discovery of leptoquarks with masses up to 2–3 TeV depending on their couplings to fermions. It is interesting to notice that the single leptoquark searches not only enlarge the reach of a collider like the LHC, but also allows to study the Yukawa couplings of the leptoquarks in a greater detail. For instance, from the numbers of events with e^+-jet and e^--jet we can infer whether the leptoquark

13

couples to $e^- \bar{q}$ or $e^+ \bar{q}$. From the size of the single production cross section we can also estimate κ for leptoquarks coupling to u and d quarks. Therefore, the LHC will be able to either make a detailed study of leptoquarks or improve considerably the present bounds.

ACKNOWLEDGMENTS

REFERENCES

[1] For a review see, W. Buchmüller, Acta Phys. Austr. Suppl. **XXVII**, 517 (1985).

[2] L. Abbott and E. Farhi, Phys. Lett. **B101**, 69 (1981); Nucl. Phys. **B189**, 547 (1981).

[3] See, for instance, P. Langacker, Phys. Rep. **72**, 185 (1981).

[4] S. Dimopoulos, Nucl. Phys. **B168**, 69 (1981); E. Farhi and L. Susskind, Phys. Rev. **D20**, 3404 (1979); J. Ellis *et. al.*, Nucl. Phys. **B182**, 529 (1981).

[5] J. L. Hewett and T. G. Rizzo, Phys. Rep. **183**, 193 (1989).

[6] H1 Collaboration, C. Adloff *et al.*, preprint DESY 97-024 (hep-ex/9702012); ZEUS Collaboration, J. Breitweg *et al.*, preprint DESY 97-025 (hep-ph/9702015).

[7] ALEPH Collaboration, D. Decamp *et al.*, Phys. Rep. **216**, 253 (1992); L3 Collaboration, O. Adriani *et al.*, Phys. Rep. **236**, 1 (1993); OPAL Collaboration, G. Alexander *et al.*, Phys. Lett. **B263**, 123 (1991).

[8] DELPHI Collaboration, P. Abreu *et al.*, Phys. Lett. **B316**, 620 (1993).

[9] CDF Collaboration, F. Abe *et al.*, hep-ex/9708017; DØ Collaboration, B. Abbott *et al.*, Fermilab-Pub-97/252-E (hep-ex/9707033)

[10] ZEUS Collaboration, M. Derrick *et al.*, Phys. Lett. **B306**, 173 (1993); H1 Collaboration, I. Abt *et al.*, Nucl. Phys. **B396**, 3 (1993); H1 Collaboration, S. Aid *et al.*, Phys. Lett. **B369**, 173 (1996).

[11] O. J. P. Éboli and A. V. Olinto, Phys. Rev. **D38**, 3461 (1988); J. L. Hewett and S. Pakvasa, *ibid.* **37**, 3165 (1988); J. Ohnemus, S. Rudaz, T. F. Walsh, and P. Zerwas, Phys. Lett. **B334**, 203 (1994); J. Blümlein, E. Boos, and A. Krykov, hep-ph/9610408; M. Krämer, *et al.*, Phys. Rev. Lett. **79**, 341 (1997); J. L. Hewett and T. Rizzo, hep-ph/9703337; T. Rizzo, hep-ph/9609267.

[12] W. Buchmüller, R. Rückl, and D. Wyler, Phys. Lett. **B191**, 442 (1987).

[13] J. Wudka, Phys. Lett. **B167**, 337 (1986); M. A. Doncheski and J. L. Hewett, Z. Phys. **C56**, 209 (1992); J. Blümlein, E. Boos, and A. Pukhov, Rev. Mod. Phys. **A9**, 3007 (1994); C. Friberg, E. Norrbin, and T. Sjöstrand, Phys. Lett. **B403**, 329 (1997); Z. Kunszt and W. J. Stirling, Z. Phys. **C75**, 453 (1997); J. Kalinowski *et al.*, hep-ph/9703288; J. Blümlein, E. Boos, and A. Krykov, hep-ph/9608483; T. Plehn *et al.*, hep-ph/9703433; J. Blümlein, hep-ph/9703287.

[14] J. L. Hewett and T. G. Rizzo, Phys. Rev. **D36**, 3367 (1987); J. L. Hewett and S. Pakvasa Phys. Lett. **B227**, 178 (1987); J. E. Cieza and O. J. P. Éboli, Phys. Rev. **D47**, 837 (1993); J. Blümein and R. Rückl, Phys. Lett. **B304**, 337 (1993); J. Blümlein and E. Boos, Nucl. Phys. **B37** (Proc. Suppl.), (1994) 181; C. G. Papadopoulos, hep-ph/9703372; J. Blümlein, E. Boos, and A. Krykov, Phys. Lett. **B392**, 150 (1997); M. S. Berger, hep-ph/9609517; M. A. Doncheski and S. Godfrey, hep-ph/9608368.

[15] F. Cuypers, Int. J. Mod. Phys. **A11**, 1627 (1996); F. Cuypers, P. H. Frampton, and R. Rueckl, Phys. Lett. **B390**, 221 (1997).

[16] O. J. P. Éboli *et al.*, Phys. Lett. **B311**, 147 (1993); H. Nadeau and D. London, Phys. Rev. **D47**, 3742 (1993); M. A. Doncheski and S. Godfrey, Phys. Rev. **D51**, 1040 (1995); T. M. Aliev, E. Iltan, and N. K. Pak, Phys. Rev. **D54**, 4263 (1996); F. Cuypers, Nucl. Phys. **B474**, 57 (1996); M. A. Doncheski and S. Godfrey, hep-ph/9612385.

[17] G. Bélanger, D. London, and H. Nadeau, Phys. Rev. **D49**, 3140 (1994).

[18] T. Sjöstrand, Computer Phys. Commun. **82**, 74 (1994).

[19] E. Tsesmelis, ATLAS internal note PHYS-NO-029; A. d'Avella, ATLAS internal note PHYS-NO-026; B. Dion *et al.*, preprint LAVAL-PHY-96-17 (hep-ph/9701285).

[20] O. Shanker, Nucl. Phys. **B204**, 375 (1982).

[21] W. Buchmüller and D. Wyler, Phys. Lett. **B177**, 377 (1986); J. C. Pati and A. Salam, Phys. Rev. **D10**, 275 (1974).

[22] M. Leurer, Phys. Rev. Lett. **71**, 1324 (1993); Phys. Rev. D**49**, 333 (1994).

[23] P. Langacker, Phys. Lett. **B256**, 277 (1991); P. Langacker, M. Luo, and A. K. Mann, Rev. Mod. Phys. **64**, 87 (1992).

[24] G. Bhattacharyya, J. Ellis, and K. Sridhar, Phys. Lett. **B336**, 100 (1994); erratum *ibid.* **B338**, 522 (1994).

[25] O. J. P. Éboli, M. C. Gonzalez-Garcia, and J. K. Mizukoshi, Nucl. Phys. **B443**, 20 (1995); Phys. Lett. **B396**, 238 (1997).

[26] S. Davidson, D. Bailey, and A. Campbell, Z. Phys. **C61**, 613 (1994).

[27] J. Botts *et al.*, Phys. Rev. D**51**, 4763 (1995).

[28] This cut on the hard scattering partons is not physical, however, it increases the efficiency of the Monte Carlo without affecting the high p_T distribution of the final leptons and jets.

[29] In our analyses we generated a set of off-shell Z events, with invariant mass larger than 200 GeV, in order to study the tail of the e^+e^- invariant mass distribution.

leptoquark	decay	branching ratio	$\kappa 4\pi \alpha_{\mathrm{em}}$
S_{1L}	$e^+\bar{u}$	50%	$\frac{g_{1L}^2}{2}$
S_{1R}	$e^+\bar{u}$	100%	$\frac{g_{1R}^2}{2}$
$\tilde{S}_{1R}$	$e^+\bar{d}$	100%	$\frac{\tilde{g}_{1R}^2}{2}$
S_3^+	$e^+\bar{d}$	100%	g_3^2
S_3^0	$e^+\bar{u}$	50%	$\frac{g_3^2}{2}$
R_{2L}^1	$e^-\bar{u}$	100%	$\frac{h_{2L}^2}{2}$
R_{2R}^1	$e^-\bar{u}$	100%	$\frac{h_{2R}^2}{2}$
R_{2R}^2	$e^-\bar{d}$	100%	$\frac{h_{2R}^2}{2}$
$\tilde{R}_2^1$	$e^-\bar{d}$	100%	$\frac{\tilde{h}_{2L}^2}{2}$

TABLE I. Leptoquarks that can be observed through their decays into a $e^\pm$ and a jet and the correspondent branching ratios into this channel. We also show the relation between the leptoquark Yukawa coupling and the parameter κ used in PYTHIA.

Process	σ_{bare} (nb)	σ_{pair} (fb)
$q_i q_j \rightarrow q_i q_j$	$1.0\ 10^2$	$4.8\ 10^2$
$q_i \bar{q}_i \rightarrow q_k \bar{q}_k$	1.8	$1.2\ 10^2$
$q_i \bar{q}_i \rightarrow gg$	1.6	2.3
$q_i g \rightarrow q_i g$	$6.2\ 10^2$	$1.0\ 10^3$
$gg \rightarrow q_k \bar{q}_k$	$25.$	$1.2\ 10^3$
$gg \rightarrow gg$	$6.9\ 10^2$	$5.5\ 10^2$

TABLE II. Background processes included in the QCD class and their respective cross sections. To obtain σ_{bare} we required that the hard scattering process has $p_T > 100$ GeV; for σ_{pair} we further demanded that the $e^{\pm}$ have $p_T > 50$ GeV.

Process	σ_{bare} (pb)	σ_{pair} (fb)	ϵ_{12}	ϵ_{123}
$q_i \bar{q}_i \rightarrow g\gamma$	74.	0.14	0	0
$q_i \bar{q}_i \rightarrow gZ$	95.	$9.2 \ 10^2$	1%	0.8%
$q_i \bar{q}_j \rightarrow gW^\pm$	$2.2 \ 10^2$	8.8	0	0
$q_i \bar{q}_i \rightarrow \gamma Z$	1.4	16.	0.6%	0.4%
$q_i \bar{q}_j \rightarrow \gamma W^\pm$	1.1	$6.6 \ 10^{-3}$	0	0
$q_i \bar{q}_i \rightarrow ZZ$	1.4	29.	0.8%	0.2%
$q_i \bar{q}_j \rightarrow ZW^\pm$	2.9	37.	1.2%	0.4%
$q_i \bar{q}_i \rightarrow W^+ W^-$	6.8	38.	4.3%	4.3%
$q_i g \rightarrow q_i \gamma$	$6.1 \ 10^2$	3.5	0	0
$q_i g \rightarrow q_i Z$	$5.5 \ 10^2$	$5.4 \ 10^3$	0.8%	0.2%
$q_i g \rightarrow q_k W^\pm$	$1.4 \ 10^3$	$2.8 \ 10^2$	0.25%	0.25%

TABLE III. Background processes included in the electroweak class and their respective cross sections with the same cuts used in Table II. We also exhibit the fraction of events ϵ_{12} (ϵ_{123}) that survive the cuts C1 and C2 (C1, C2, and C3); see text.

Process	σ_{bare} (pb)	σ_{pair} (fb)	ϵ_{12}	ϵ_{123}
$q_i q_j \rightarrow t q_k$	40.	11.	0.85%	0.01%
$q_i \bar{q}_i \rightarrow t\bar{t}$	0.40	$2.0\ 10^2$	0.40%	0.39%
$gg \rightarrow t\bar{t}$	$2.9\ 10^2$	$1.4\ 10^3$	75%	3.5%

TABLE IV. Background processes due to top quark production and their respective cross sections with the same cuts used in Table II. We also exhibit the fraction of events ϵ_{12} (ϵ_{123}) that survive the cuts C1 and C2 (C1, C2, and C3).

ℓq coupling	$M_{\text{lq}} = 500$ GeV	1000 GeV	1500 GeV	2000 GeV	2500 GeV
$e^{\pm} u$	$5.1\ 10^2$	27.	4.1	0.98	0.29
$e^{\pm} d$	$2.9\ 10^2$	14.	2.2	0.55	0.18

TABLE V. Total cross section in fb for the single production of a leptoquark that couples only to pair ℓq for several leptoquark masses. We required that the produced $e^{\pm}$ have $p_T > 50$ GeV, and that the scattering process has $p_T > 100$ GeV.

process	$M_{lq} = 500$ GeV	1000 GeV	1500 GeV	2000 GeV
$q\bar{q}$ fusion	86.	1.9	0.10	$2.7\ 10^{-3}$
gg fusion	$4.9\ 10^{2}$	6.3	0.25	$1.5\ 10^{-2}$

TABLE VI. Total cross section in fb for the pair production of leptoquarks, requiring that the produced $e^{\pm}$ have $p_T > 50$ GeV, and that the hard scattering process has $p_T > 100$ GeV.

M_{lq} (GeV)	ΔM (GeV)
300	50
500	50
1000	150
1500	200
2000	200
2500	300

TABLE VII. Invariant mass bins used in our analyses as a function of the leptoquark mass.

leptoquark	$\mathcal{L} = 10$ fb^{-1}	$\mathcal{L} = 100$ fb^{-1}
S_{1L} and S_3^0	1.1	1.5
S_{1R}, $\tilde{S}_{1R}$, R_{2L}^1, R_{2R}^2, and $\tilde{R}_2^1$	1.3	1.7

TABLE VIII. 95% CL limits on the leptoquark masses in TeV that can be obtained from the search for leptoquark pairs for two integrated luminosities.
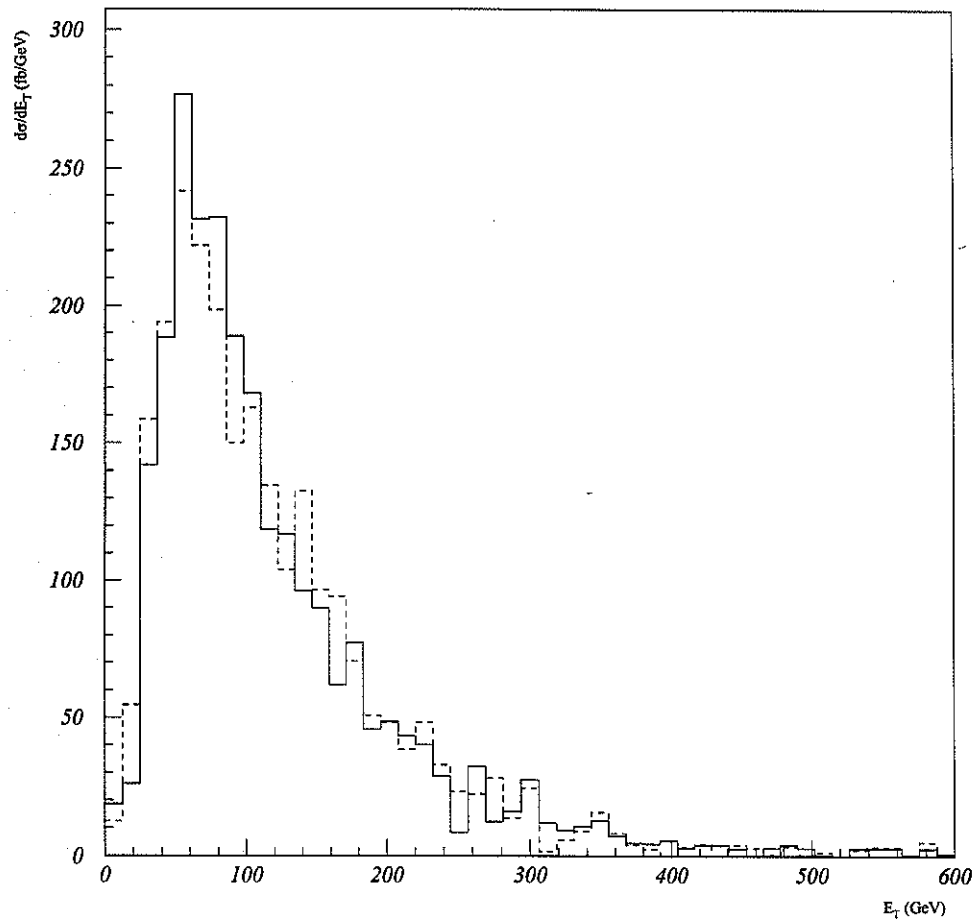
FIG. 1. Hadronic transverse energy deposited in a cone of size $\Delta R = 0.7$ around the direction of the e_1 (solid line) and the e_2 (dashed line) in QCD events.

23
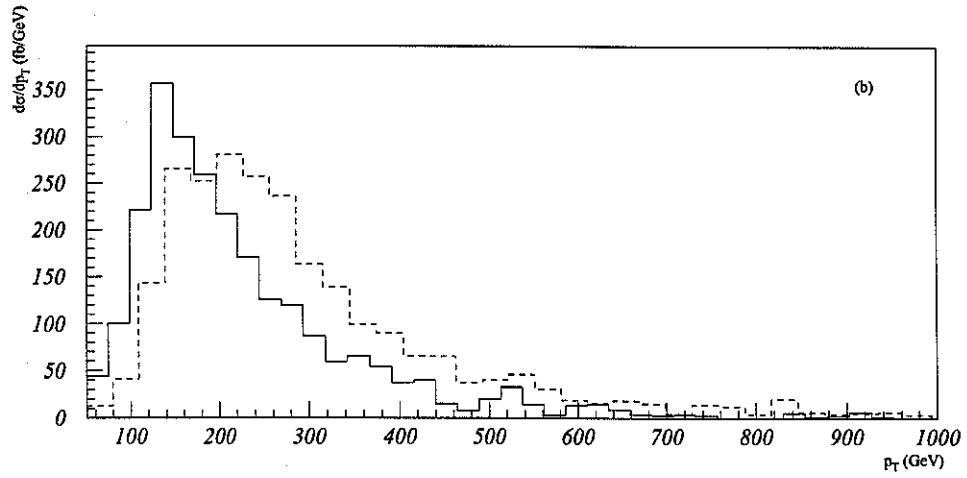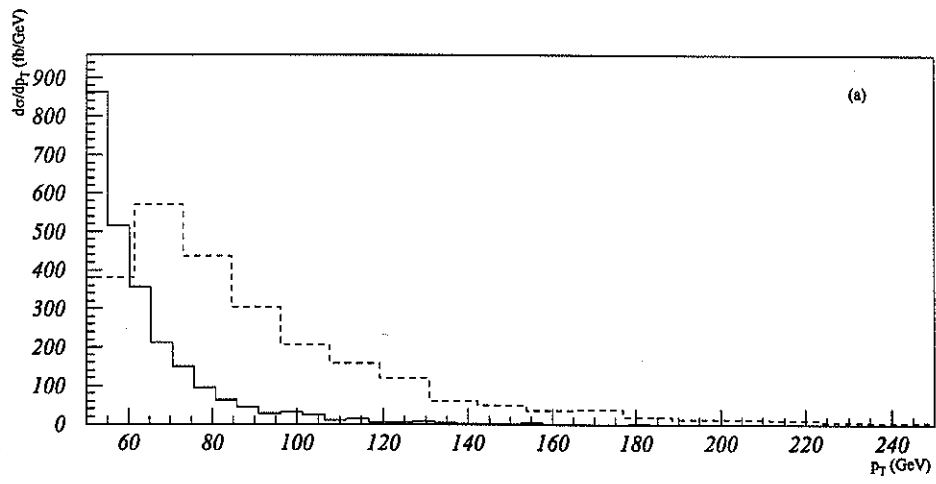
FIG. 2. For QCD events: (a) the dashed (solid) line stands for the p_T distribution of e_1 (e_2); (b) the dashed (solid) line stands for the p_T distribution of j_1 (j_2).

24
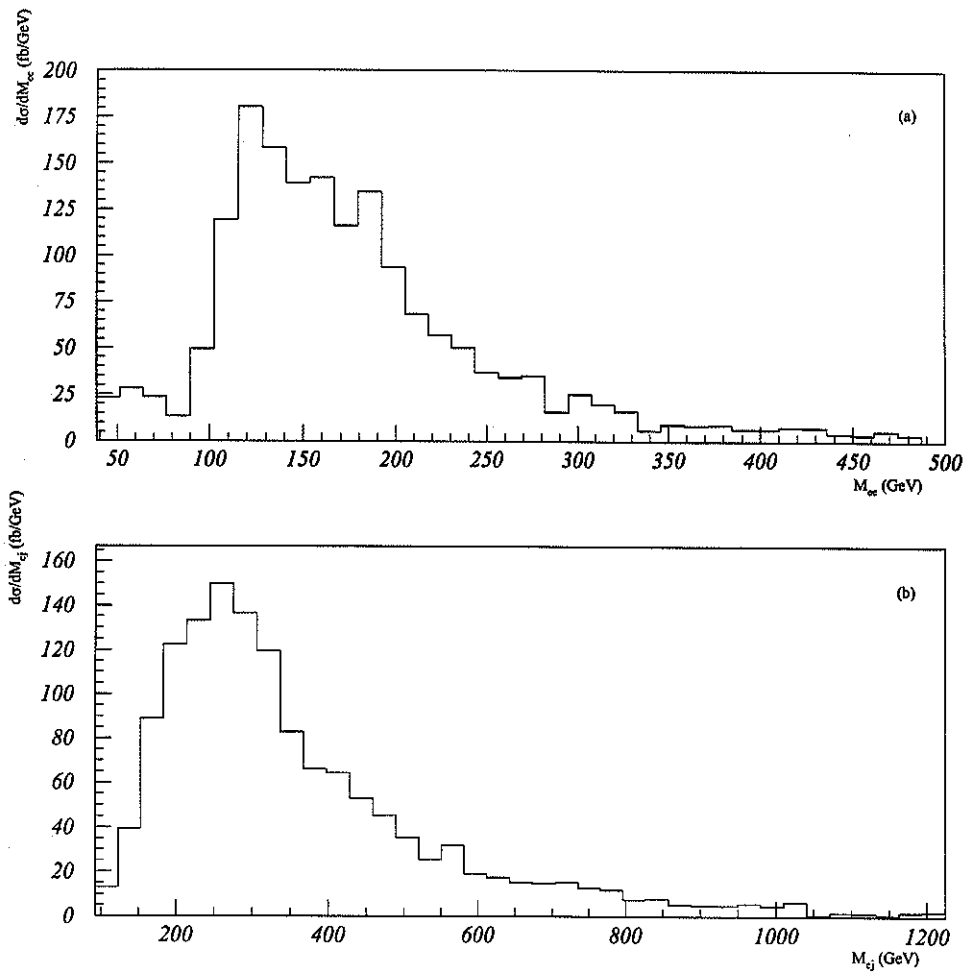
FIG. 3. For QCD events: (a) $e_1 e_2$ invariant mass distribution; (b) $e^{\pm}$-jet invariant mass spectrum adding the 4 possible combinations.
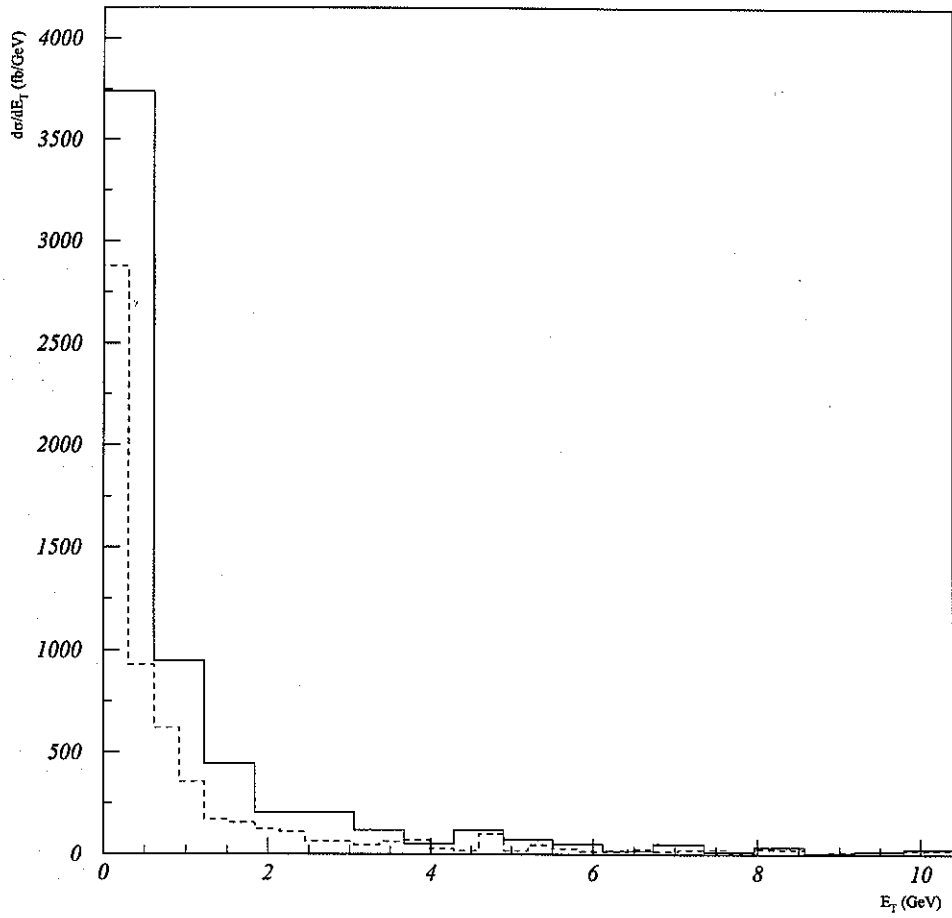
FIG. 4. The same distributions of Fig. 1 for electroweak events.
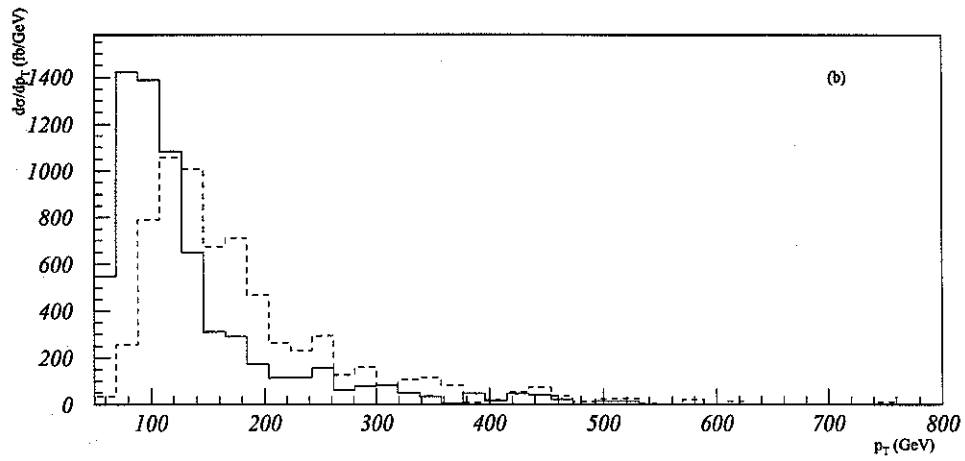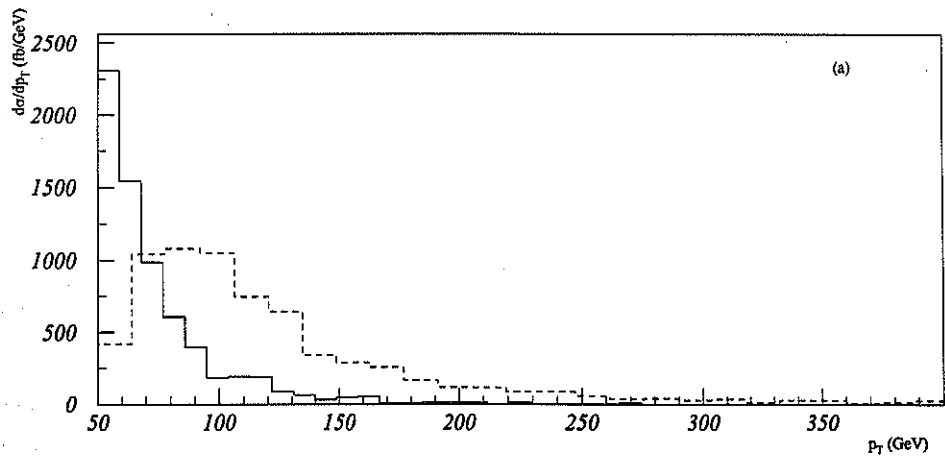
FIG. 5. The same distributions of Fig. 2 for electroweak events.

27
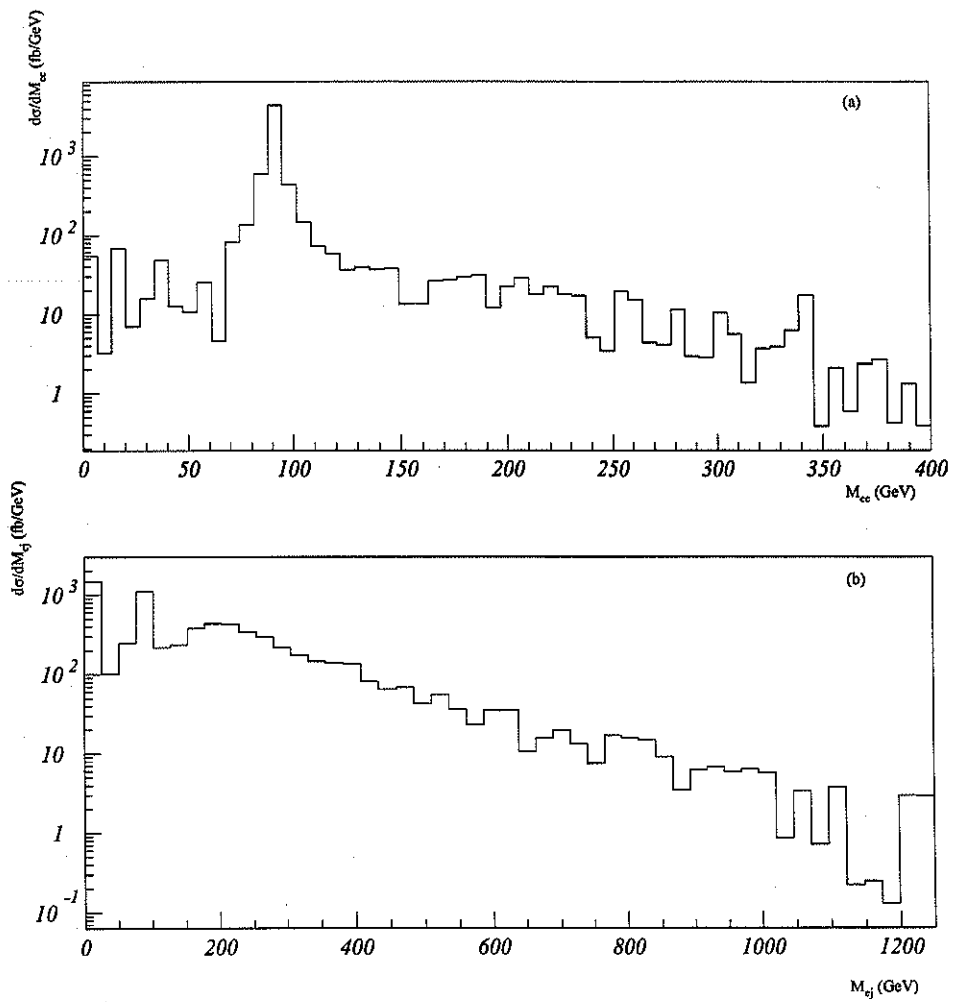
FIG. 6. The same distribution of Fig. 3 for electroweak events.
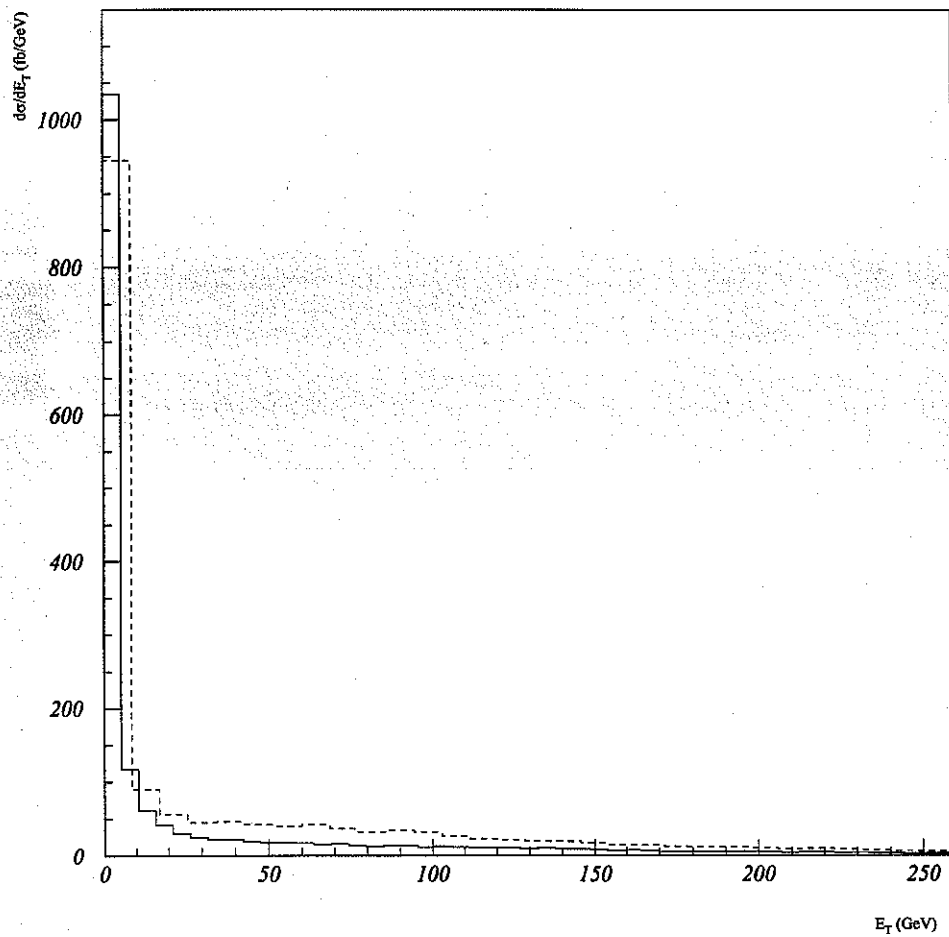
FIG. 7. The same distribution of Fig. 1 for top production.

29
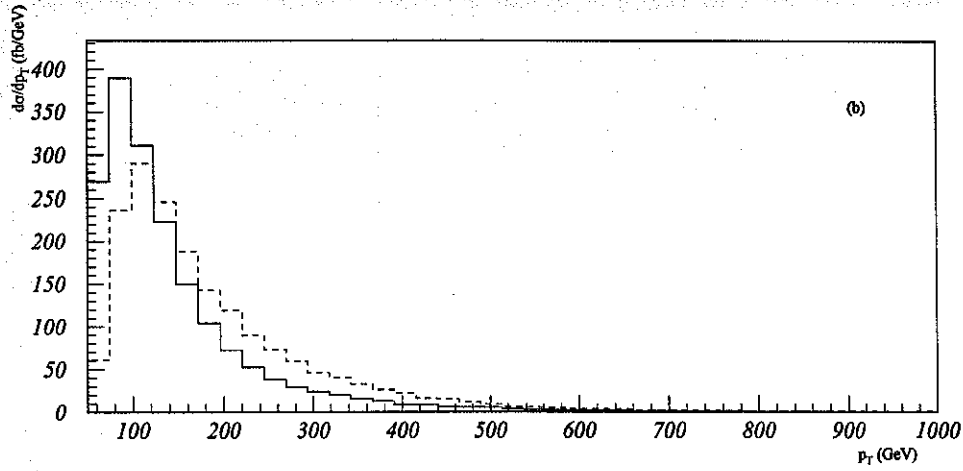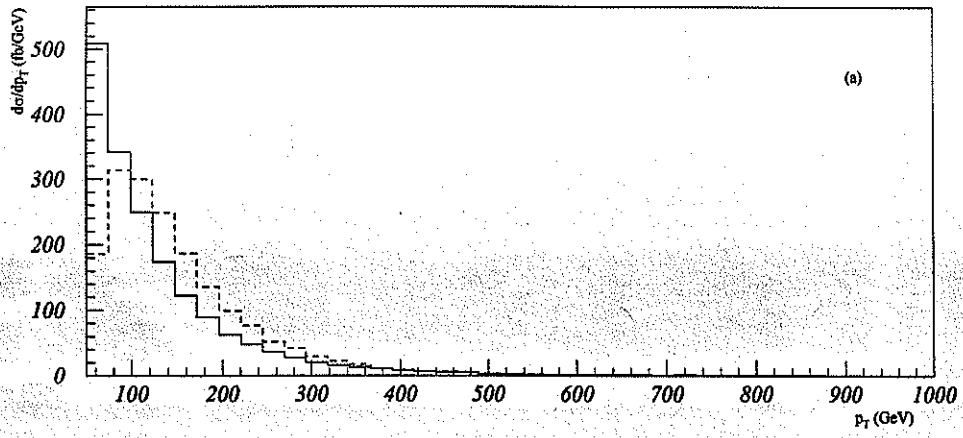
FIG. 8. The same distribution of Fig. 2 for top production.
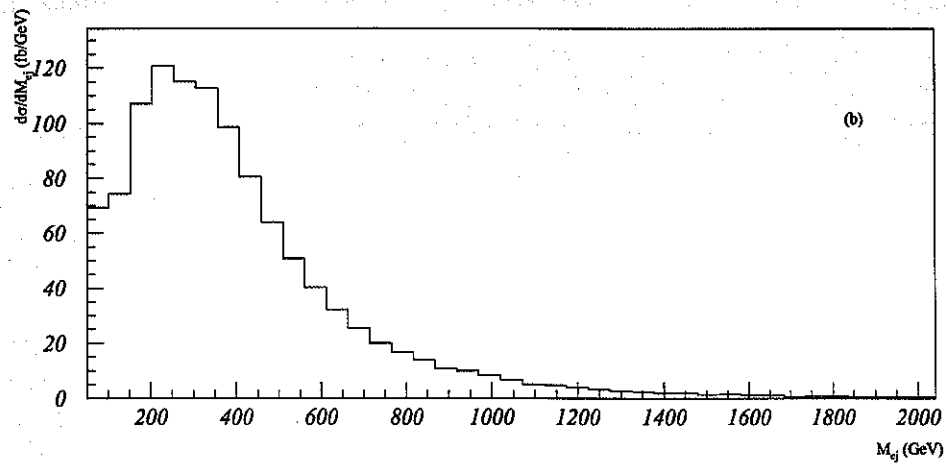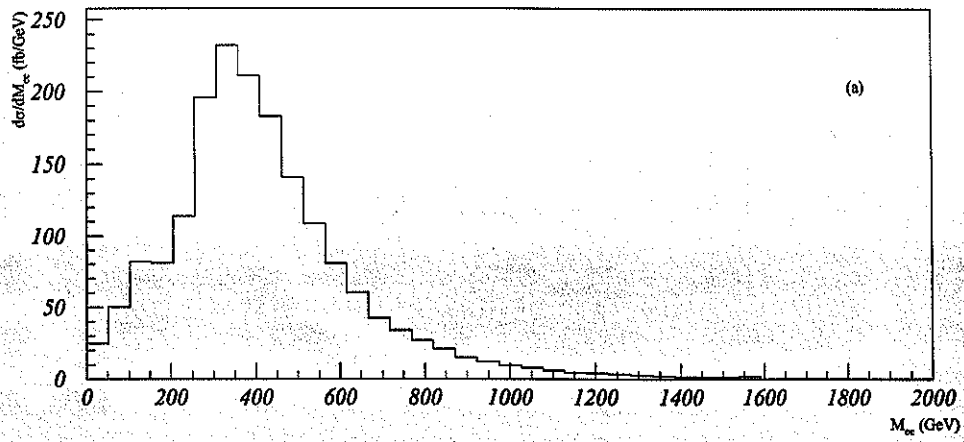
FIG. 9. The same distribution of Fig. 3 for top production.
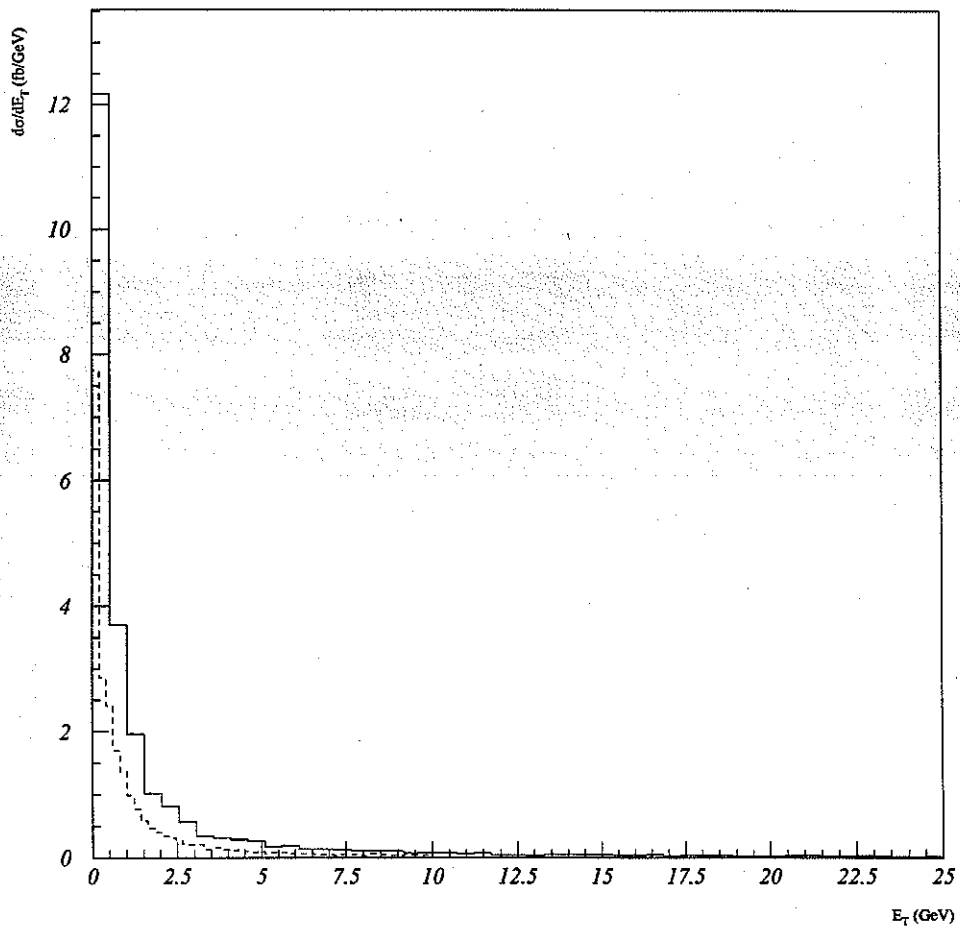
FIG. 10. The same distribution of Fig. 1 for the single production of $e^+\bar{u}$ leptoquarks of mass 1 TeV.

32
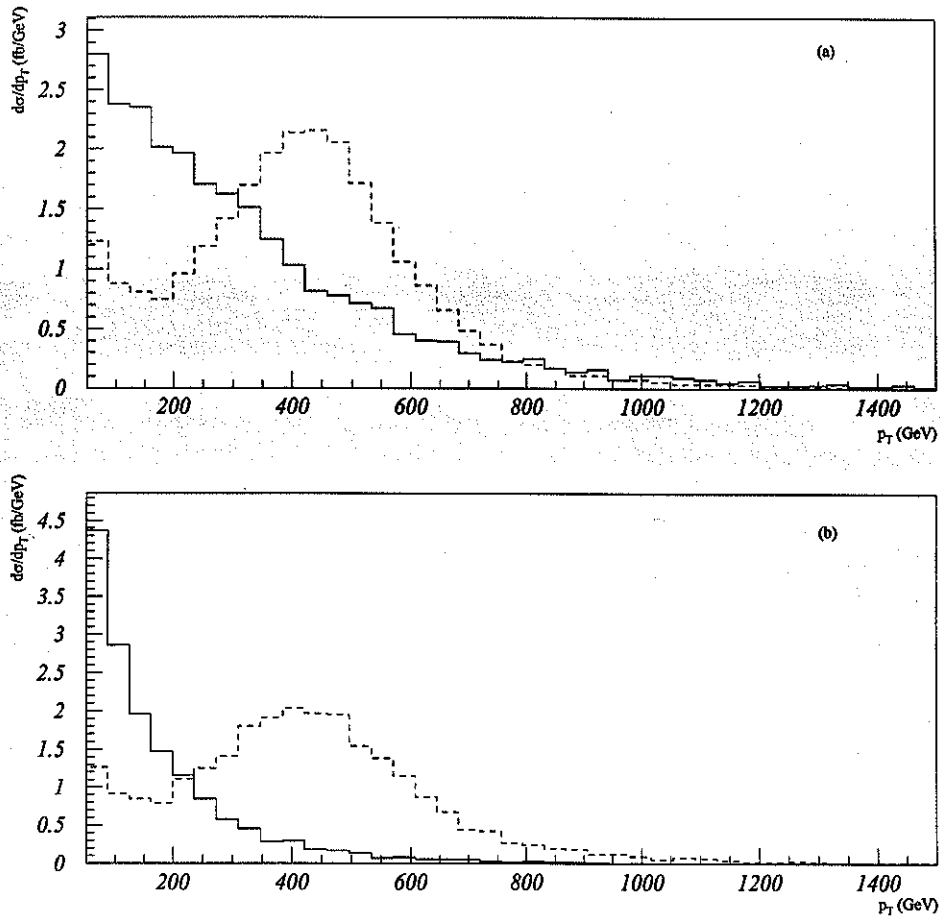
FIG. 11. The same distribution of Fig. 2 for the single production of $e^+\bar{u}$ leptoquarks of mass 1 TeV.
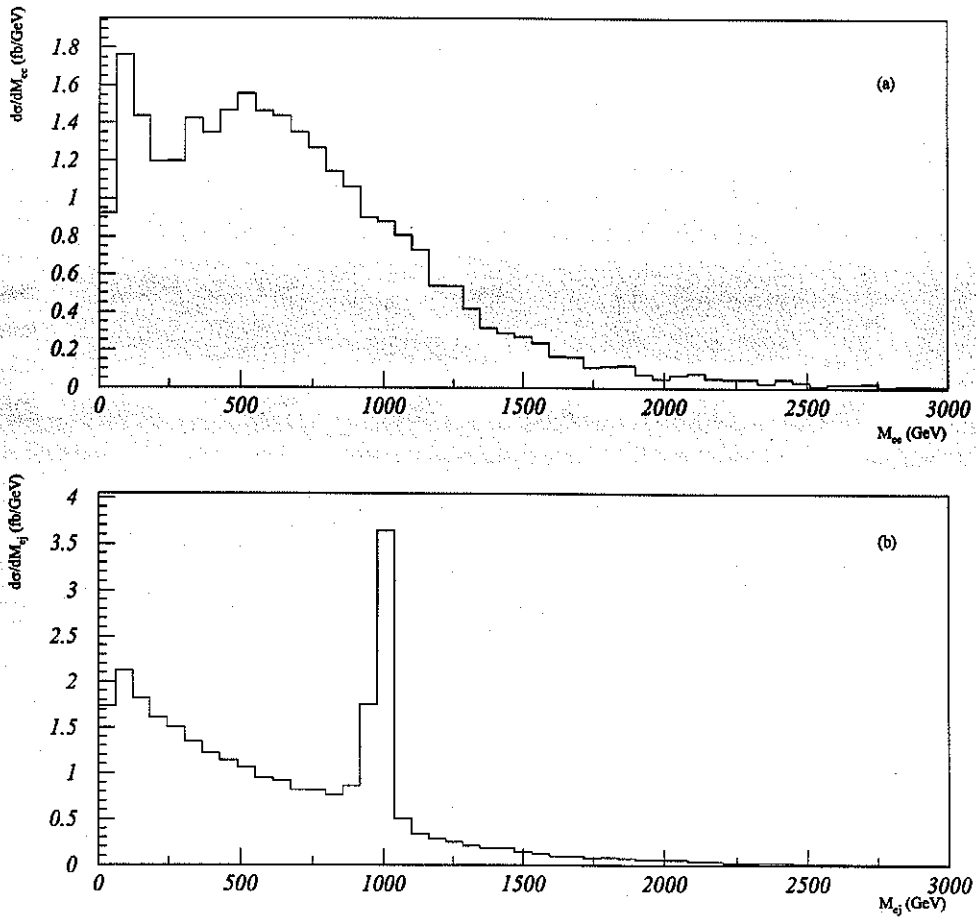
FIG. 12. The same distribution of Fig. 3 for the single production of $e^+\tilde{u}$ leptoquarks of mass 1 TeV.

34
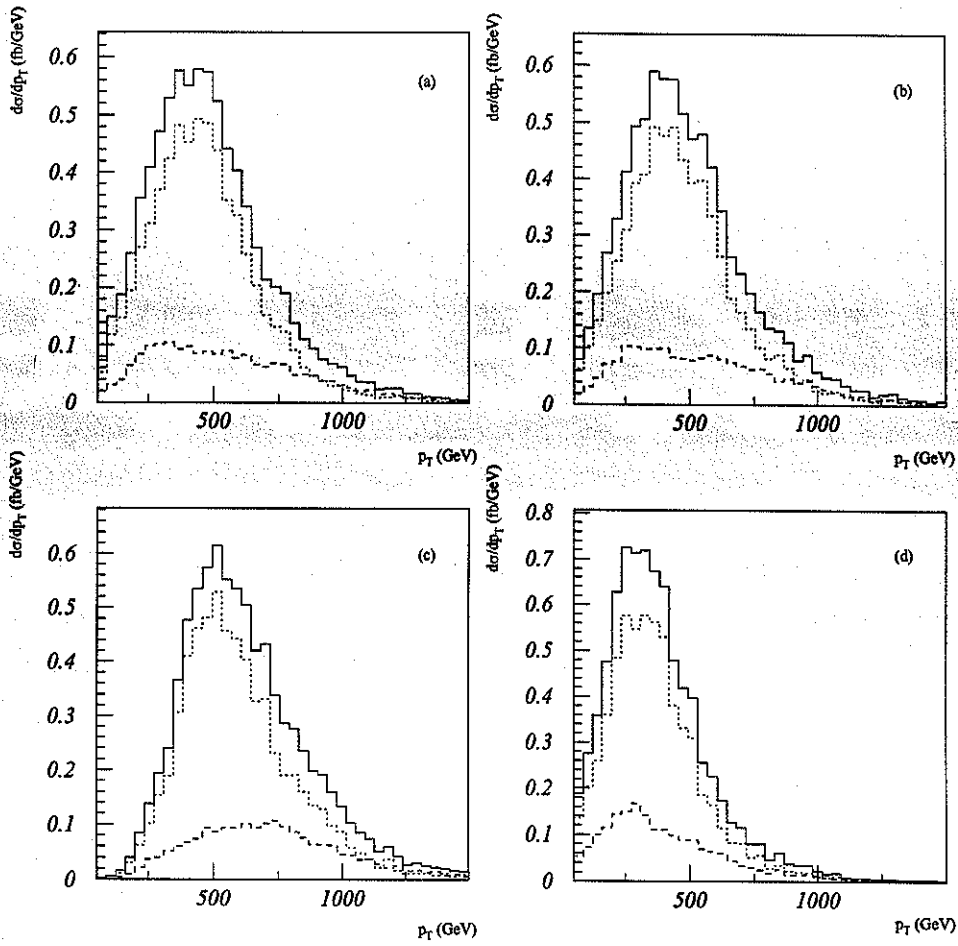
FIG. 13. p_T distribution of (a) e_1; (b) e_2; (c) j_1; (d) j_2; in the pair production of $e^+\bar{u}$ leptoquarks of mass 1 TeV. The dashed (dotted) line stands for the $q\bar{q}$- (gg-) fusion contribution while the solid line represents the total distribution.
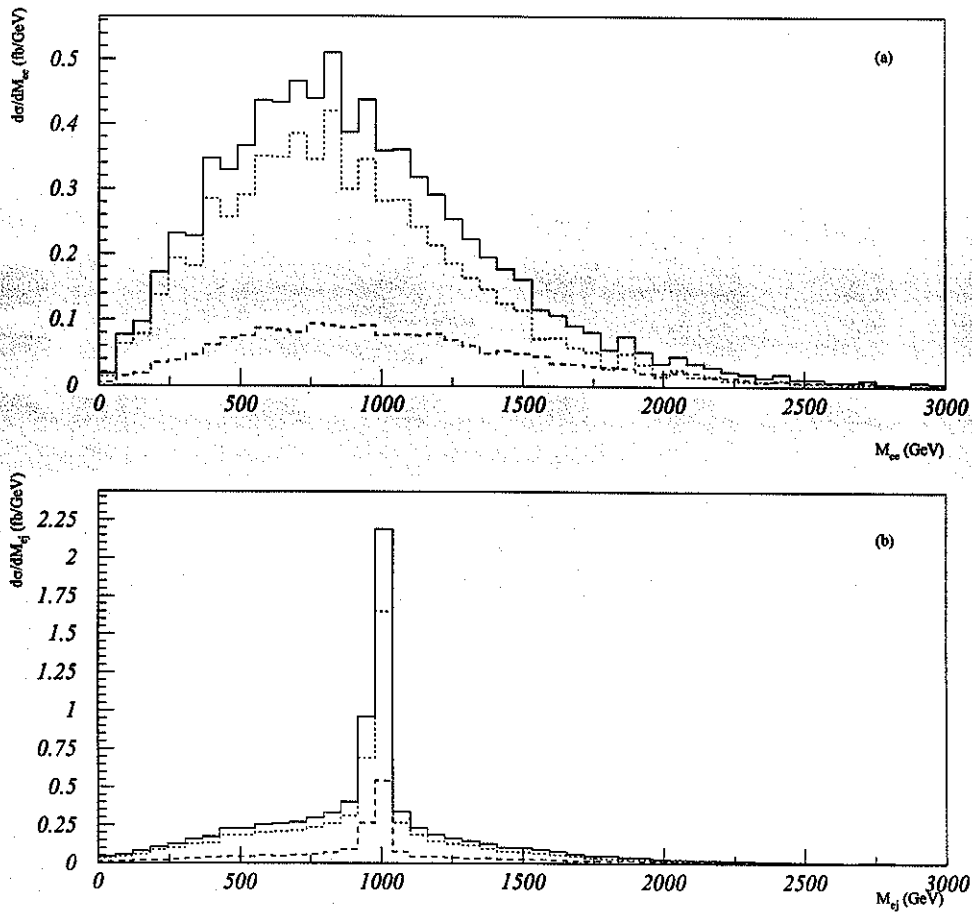
FIG. 14. (a) e^+e^- invariant mass distribution; (b) $e^{\pm}$-jet invariant mass spectrum adding the 4 possible combinations for pair production of $e^+\bar{u}$ leptoquarks with mass $M_{lq} = 1$ TeV. We use the conventions of Fig. 13.
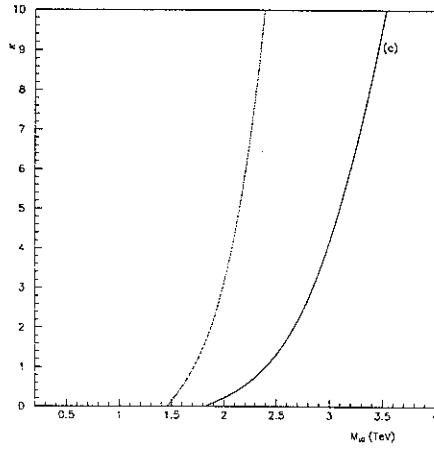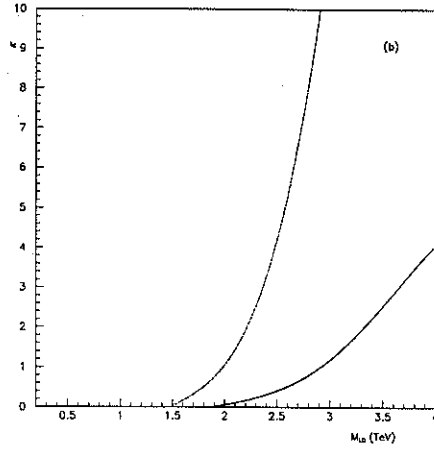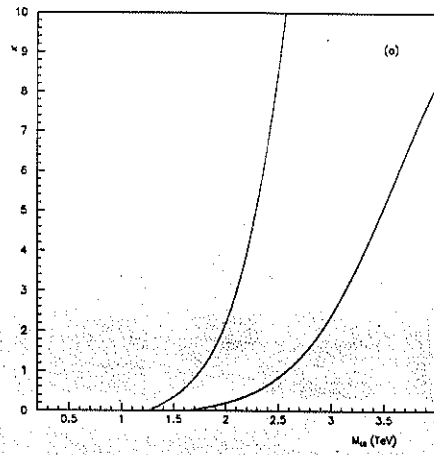
FIG. 15. 95% excluded regions in the plane κ–M_{lq} from the single leptoquark analysis for an integrated luminosity of $10/100\,\mathrm{fb}^{-1}$ (solid/dotted line) and the leptoquarks: (a) S_{1L} and S_3^0; (b) S_{1R}, R_{2L}^1, and R_{2R}^1; (c)S_3^+, R_{2R}^2, $\tilde{R}_2^1$, and $\tilde{S}_{1R}$.

37